Deposition of aminosilane coatings on porous Al_2O_3 microspheres by means of dielectric barrier discharges

Article type: Full Paper

Deposition of aminosilane coatings on porous Al_2O_3 microspheres by means of dielectric barrier discharges

Marta Garzia Trulli*, Nathalie Claes, Judith Pype, Sara Bals, Kitty Baert, Herman Terryn, Eloisa Sardella, Pietro Favia, Annick Vanhulsel*

_____

M. Garzia Trulli, Prof. P. Favia
Department of Chemistry, University of Bari "Aldo Moro", Via Orabona 4, 70126 Bari, Italy
E-mail: marta.garziatrulli@uniba.it
N. Claes, Prof. S. Bals
Electron Microscopy for Materials Science (EMAT), University of Antwerp, Groenenborgerlaan 171, 2020 Antwerp, Belgium
J. Pype
Laboratory of Adsorption and Catalysis (LADCA), Department of Chemistry, University of Antwerp, CDE, Universiteitsplein 1, 2610 Wilrijk, Belgium
Ing. K. Baert, Prof. H. Terryn
Research Group Electrochemical and Surface Engineering, Vrije Universiteit Brussel, Pleinlaan 2, 1050 Brussels, Belgium
Dr. E. Sardella, Prof. P. Favia
CNR-Institute of Nanotechnology (CNR-NANOTEC), URT Bari c/o Department of Chemistry, University of Bari, via Orabona 4, Bari 70126, Italy
Dr. Ir. A.Vanhulsel
Materials Department, Flemish Institute for Technological Research (VITO), Boeretang 200, 2400 Mol, Belgium
SIM (Strategic Initiative Materials Flanders) vzw, Zwijnaarde, Belgium
E-mail: annick.vanhulsel@vito.be

_____

Advances in the synthesis of porous microspheres and in their functionalization are increasing the interest in applications of alumina. This paper deals with coatings plasma deposited from 3-Aminopropyltriethoxysilane by means of dielectric barrier discharges on alumina porous microspheres, shaped by a vibrational droplet coagulation technique. Aims of the work are the functionalization of the particles with active amino groups, as well as the evaluation of their surface coverage and of the penetration of the coatings into their pores. A multi-diagnostic approach was used for the chemical/morphological characterization of the particles. It was found that 5 min exposure to plasma discharges promotes the deposition of homogeneous coatings onto the microspheres and within

their pores, down to 1 µm.

1 Introduction

Porous ceramic particles based on metal oxides are facing continuously growing applications, particularly those composed of silica and alumina, due to their unique properties: high surface area, good mechanical, thermal and chemical stability, valuable catalytic activity, as well as the possibility of fabricating them in tunable micro and nano dimensions and pore sizes.[1,2] In particular, their permeability to various gases and liquids makes ceramics with well-developed open pores appealing and widely employable in many technological fields, as filters for molten metals, catalyst carriers, high temperature insulators and lightweight structural materials.[3-6] Furthermore, mesoporous nano ceramic particles are excellent candidates also for drug delivery and other biomedical applications.[7-10]

It is important to highlight that, beside the favorable texture (i.e. appropriate pore size distributions and high surface area), the application of alumina in different fields depends on its surface chemical characteristics. An acidic or basic character can be imparted during the synthesis, as in the case of a class of aluminum oxides known as transition alumina by changing the degree of surface hydration and hydroxylation.[11] Moreover, the preparation of porous alumina particles functionalized with other chemical groups, such as -COOH and -NH_2 ones, can further extend their range of applications. For instance, carboxylate-alumoxanes particles decorated with covalently bound carboxylate groups can be synthetized through the reaction of bohemite with carboxylic acids.[12] The functionalization of ceramic particles with amino groups can be performed prevalently by using classical wet reactive deposition methods of aminosilane coupling agents,[13,14] like 3-Aminopropyltriethoxysiloxane (APTES), in order to get organic–inorganic hybrid porous materials.[1,15,16] All these methods make use of solvents,[15,17,18] however, in view of the industrial

scale-up and of the economics of the process, the development of alternative solvent-less methods would be appreciated. Among others, plasma technologies have fully proved to be flexible, one-shot, solvent-less and contaminant-free functionalization methods of materials in a great number of established and future applications.[19,20]

In the last few years there has been a growing interest in the plasma treatments of micro and nano particles,[21-25] including inorganic ceramic powders,[26-28] both at low (LP) and atmospheric pressure (AP). As reported in literature, the colloidal stability of alumina powders can be enhanced with AP plasma treatments in air,[29] and the stability of TiO_2 particles in water can be increased with the LP plasma deposition of coatings from acrylic acid.[30] Ultrathin adhesive films LP plasma deposited from pyrrole at the surface of alumina nanoparticles have been studied by D. Shi et al.[31]
Very few studies are reported in literature about the solvent-less functionalization of ceramic particles with silane compounds, even though the AP Plasma Enhanced Chemical Vapor Deposition (PE-CVD) of flat substrates with APTES has been proved to be an efficient and innovative alternative functionalization method.[32,33]
The AP PE-CVD surface modification of fine alumina powders was carried out with Tetraethoxysilane (TEOS) in a circulating fluidized bed plasma reactor, in order to deposit organic silicone-like films SiOxCyHz.[34] M. Lazghab et al.[35] have studied the hydrophobization of highly porous silica powders in a fluidized-bed reactor with Glycidoxypropyltrimethoxysilane (GPTMS) and APTES, using particles with a known amount of coupling reagent as "reagent-carrier". Tetrachlorosilane and APTES have been used as silicon precursor and surface modifier, respectively, for a two-step preparation of modified silica nanopowders in an AP microwave plasma.[36]

Plasma technology has proved to be an efficient approach not only for the surface modification of materials, but also for the internal surface modification of porous channels. A. Choukourov et al.[37] reported an AP PE-CVD process from n‑Hexane on mesoporous films of titanium

nanoparticles, as well as the penetration of the hydrocarbon coating within the porous structure. The effect of a plasma process inside the intra-particle volume of porous alumina was analyzed by Roland et al.[38] to evaluate the potential of combining cold plasma and in situ heterogeneous plasma catalysis for the oxidation of volatile organic compounds in gas cleaning applications. A two steps process has been recently reported for the internal surface modification in one-dimensional channels of mesoporous silica particles, which combines an AP DBD O_2 plasma treatment with a further conventional functionalization approach with APTES. The plasma activation of the silanol groups at the surface of the channels allowed the grafting of a large amount of amine groups. However, the second step required the use of solvents and at least 2 h to be realized.[39]

Most of the studies listed above have used several characterization techniques to characterize the coatings deposited at the surface of the particles. Very few studies, though, have been performed to characterize the functionalization inside the pores of the particles.

The main goal of this study is to functionalize Al_2O_3 microspheres with two levels of porosity, about 0.7 % and about 37 % of total porosity, at the external surface as well as within the pores of the particles, through an AP DBD process. APTES vapors were used to feed the discharges in order to plasma deposit a siloxane layer with active amino groups. The effect of treatment time, input power and chemical composition of the gas feed mixture were studied. X-ray photoelectron spectroscopy (XPS) and Energy Dispersive X-ray spectroscopy (EDX) analyses were performed to characterize the coating deposited at the surface of the microspheres. High Angle Annular Dark Field Scanning Transmission Electron Microscopy (HAADF-STEM) was also performed, to investigate the homogeneous distribution of the coating on the whole external surface of the particles, as well as the efficiency of its penetration inside the pores.

2 Experimental Section

2.1 Materials

Monodisperse alumina microspheres, with two levels of porosity, were used as substrate material. APTES (≥ 99% purity, Sigma-Aldrich, Belgium) was selected as feed precursor for the plasma deposition process; N_2 (Air Liquide, 99.997%) or Ar (Air Products, 99.998%) as carrier gas. Double polished silicon substrates were used for FT-IR analysis and for the measurements of film thickness. Orange II sodium salt (Sigma-Aldrich, Belgium) was used as anionic dye for quantification of the amino groups.

2.2 Synthesis of alumina microspheres

Monodisperse alumina microspheres were shaped by make use the vibrational droplet coagulation technique, with a Spheridisator M apparatus (Brace GmbH, Germany).[40] This technique makes use of the ionotropic gelation of sodium alginate, when in contact with a divalent cation, e.g. $CaCl_2$. α-alumina powder was loaded in a sodium alginate solution in combination with a dispersing agent (Darvan C), in order to obtain a stable ceramic suspension. A constant pressure (500 mbar) was applied on the feed tank containing the alumina suspension, to obtain a laminar flow through the nozzle (600 µm). The flow was broken up into uniform droplets by applying a vibration with constant frequency and amplitude (350 Hz, 2500 mV). These droplets were collected and solidified in a coagulation bath containing 4 wt% $CaCl_2$. The shaped microspheres were kept in the coagulation bath overnight to complete the solidification. The microspheres were then thoroughly washed with tap water, followed by RO (Reverse Osmosis) water to remove the excess of ions, and isopropyl alcohol to reduce the capillary pressure during the drying. The samples were

dried at 100°C and sintered (1 h) at 1300°C or 1650°C (heating rate 2°C/min) under ambient air and pressure conditions.

2.3 Plasma Process

The atmospheric plasma modification of the alumina microspheres was performed in the PlasmaZone® system, a parallel plate DBD semidynamic reactor, shown schematically in Figure 1.

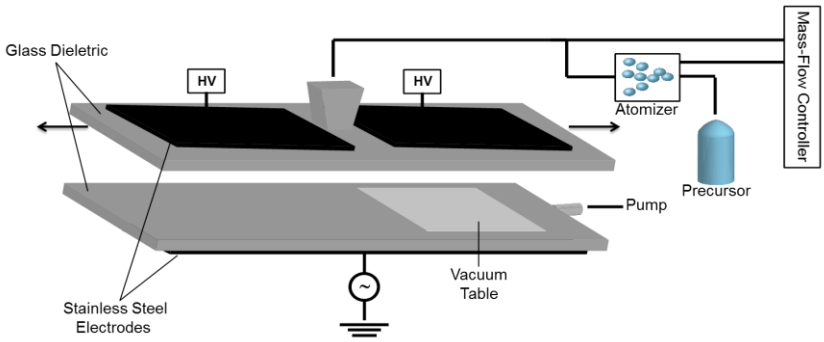

Figure 1. Schematic of the DBD plasma reactor.

The discharge was generated between two metallic stainless steel electrodes, both covered with 3.5 mm thick borosilicate glass plate used as dielectric. The high voltage (HV) electrode consists of two rectangular (9 cm × 34 cm) metallic plates. The Al_2O_3 particles (2.5 g per treatment) were placed on a 3 μm thick PVDF membrane foil on the bottom grounded electrode, equipped with a vacuum system to hold the powders in place during the plasma treatments. The top HV electrode was kept moving with a speed of 4m/min above the ground electrode to achieve homogeneous plasma treatments.[41] Two different gas flows were used for the deposition process: N_2 or Ar (carrier gas) were used to ignite and sustain the discharge at a flow rate of 20 slm; APTES was added to this flow as an aerosol produced with 1 slm of N_2 or Ar (atomizer flow) in a home-built atomizer. The precursor consumption under these conditions was 0.04 g/min. The inter-electrode gap was set at 2 mm and a fixed frequency of 1.5 kHz was optimized to ensure stable plasma operation in N_2 and Ar atmosphere. Gas curtains of carrier gas were employed to prevent air

contamination in the plasma area. The applied power, provided by an HV generator (AFS G10S-V), was varied in the range of 200 - 400 W for plasma treatments in N_2 atmosphere. For the treatments in Ar, a fixed power level of 50 W was used. Several experimental conditions were investigated to change the chemistry of treated surface, as listed in Table 1, and to study the effect of deposition time, plasma power and carrier gas. The main goal was to improve the depth of penetration and the conformality of the plasma deposited layer within the pores of the microspheres. During each pass the sample was exposed to the plasma for 5 s. Plasma treatments were carried out also on double polished silicon, in order to easily characterize the deposited films.

Table 1. Experimental conditions for plasma deposited thin coatings (f = 1.5 kHz, precursor: APTES, N_2/Ar gas flow: 20 slm).

	Deposition time [a] **[passes]**	**Power [W]**	**Carrier Gas**	**Aerosol flow [slm]**
Effect of time	10 - 30 - 60	200	N_2	1
Effect of input power	60	200 - 400	N_2	1
Effect of carrier gas	30 - 60	200/50	N_2 /Ar	0 - 1

[a] The effective exposure time of the sample to the plasma is 50, 150 and 300 s for a treatment of 10, 30 and 60 passes, respectively.

2.4 Characterization of the microspheres

The morphology inspection of the microsphere was carried out using a cold field emission scanning electron microscope (FEGSEM, Nova Nano SEM 450, FEI, USA) on samples metallized with Pt/Pd (80/20) by sputter coating (2.5 nm thick). Untreated and plasma treated microspheres were examined with extraction voltages of 10 kV. The porosity of the sintered microspheres was determined from cross section SEM images, using the image analysis software ImageJ. Thermally treated microspheres were encapsulated within an epoxy resin and cured at room temperature. Afterwards, the samples were grinded and polished. The cross sections obtained were examined at an acceleration of 5 kV.

Dynamic light scattering (DLS) was used to characterize the size distribution of the

microspheres, employing a laser diffraction system (Microtrac S3500). Approximately 0.2 g of Al_2O_3 powders were loaded in a Turbotrac autofeeder and analyzed, over a course of 10 seconds, with a TRI-LASER multi-detection system. The data was averaged over 3 measurements and analyzed with the Microtrac flex 11.0.0.3 software. The pore size distribution was measured with the mercury intrusion porosimetry test, using a Pascal 240 (Thermo Electron) porosimeter.

2.5 Chemical characterization of the coating

FT-IR and profilometry measurements were carried out on double polished silicon substrates. A commercial Vertex 70V under vacuum Bruker spectrometer was used for the acquisition of the FT-IR spectra of the plasma deposited coatings in absorbance. The thickness of the coating was quantified with a profilometer (KLA D-120 Tencor) and presented as average value of at least three measurements per sample. The plasma deposited APTES coatings had a measured growth speed of 12 ± 3 nm/min, not quite dependent on the experimental conditions used.

XPS analyses were performed with a PHI-5600ci X-ray spectrometer, using a monochromatic Al X-ray source operating at 150 W. The measurements were performed in fixed analyser transmission mode using pass energy of 187.85 eV for the survey spectra and 23.5 eV for the high-resolution spectra, with a spot size of 400 µm. A flood gun (18 mA of emission current and 40 eV of electron energy) was used for charge compensation during the analysis; the spectra were corrected for C_{1s} at 284.7 eV. The analyses were performed on the alumina microspheres supported on indium foils. C1s and N1s signals were best-fitted (MultiPak software) with four components, as follows:[42,43] C0 (285.0 ± 0.2 eV): C-C/C-R(H); C1 (286.0 ± 0.2 eV): C-N; C2 (286.6 ± 0.2 eV): C-O-R(H) /C=N; C3 (288.0 ± 0.2 eV): C=O/N-C=O; N1 (398.8 ± 0.2 eV): N=C; N2 (399.7 ± 0.2 eV): C-N; N3 (400.5 ± 0.2 eV): N-C=O; N4 (401.7 ± 0.2 eV): NH_2/NH_3^+.

A colorimetric test with the Acid Orange anionic dye was carried out in order to quantitatively determine the presence of primary amine groups in the coatings. The adsorption of the dye proceeds

via the reversible electrostatic interactions between the protonated amino groups and the negatively charged sulfonate groups of the dye, followed by the deprotonation of the amine groups under basic conditions and by the release of the dye into the solution, whose absorbance was measured to evaluate the desorbed quantity of the dye.[44,45] Untreated and plasma treated alumina microspheres were immersed in 10 ml of acid orange dye solution (40 mM) and mechanically stirred for 3 h. The samples were then intensively rinsed with an HCl solution (pH 3) to remove the unbound dye, until the washing solution was clear. Once dried in oven at room temperature for one night, a known amount of the microspheres were weighted with a microbalance and immersed in 10 ml of NaOH solution (pH 12), stirred overnight. The maximum absorbance value of the solution was then measured in the range 400 - 700 nm using an UV/VIS/NIR spectrometer (Perkin Elmer, Lambda 900). The reproducibility of the results was verified with three analyses per sample.

2.6 Morphological characterization of the coating on the microspheres

In order to visualize the coating and investigate the penetration into the alumina pores, the particles were embedded in an epoxy resin (EPO-TEK 353ND-T4) and polished until the largest cross section (middle section) was obtained. A carbon coating of 30 nm was applied. A FEI Nova 200 Nanolab Dual Beam SEM/Focused Ion Beam (FIB) system, equipped with a Ga^+ beam, was then used to prepare lamellar cross sections at the position of the interface (epoxy-Al_2O_3) with a final thinning FIB energy of 2 kV and a current of 23 pA. The energy and current values used in the different steps of the FIB procedure are reported in Table S1. The samples were investigated by HAADF-STEM and EDX. All results were obtained using a FEI Tecnai transmission electron microscope, equipped with Super-X system, operated at 200 kV.

3 Results and Discussion

The porosity of the alumina microspheres, expressed in term of percentage of void volume on the total, is influenced by the sintering temperature. From SEM analysis of the cross sections, as shown in Figure 2, the total porosity was found 37 ± 2 % for the samples sintered at 1300°C and 0.7 ± 0.2 % for those sintered at 1650°C. By increasing the sintering temperature, a decrease of the porosity level was obtained. Moreover, the SEM images in Figure 2b show that the cross section of the microspheres sintered at 1650°C is covered with lighter dots in the matrix of the α-Al_2O_3. This should be an indication of the presence of an extra crystal phase of calcium hexaluminate ($CaO.6Al_2O_3$), produced by the sintering of calcium in presence of α-alumina.[46]

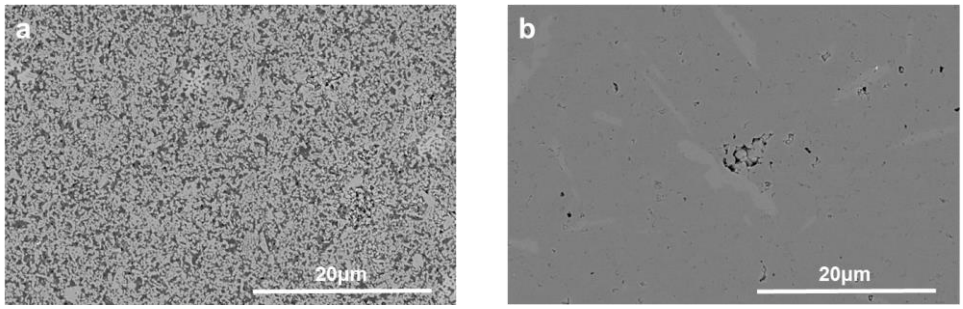

Figure 2. SEM analysis (2500x) of cross sections of microspheres at two sintering temperatures: a) 1 h at 1300°C and b) 1 h at 1650°C.

The size distribution of the spheres is correlated to the nozzle diameter, which controls the size of the droplets. As presented in an earlier work, a linear relation between the nozzle diameter and the average size of the microspheres was verified.[40] With the nozzle diameter kept constant at 600 µm, the average microsphere size measured with the DLS technique results 675 ± 5 µm for the samples sintered at 1300°C and 616 ± 5 µm for the samples sintered at 1650°C. The higher sintering temperature results in the shrinking of the spheres. The pore diameters (average weighted value), measured with the mercury intrusion porosimetry test, are 138 ± 20 nm and 38 ± 8 nm, for the samples sintered at lower and higher temperature, respectively.

Alumina microspheres were plasma treated, with the conditions summarized in Table 1, in the DBD reactor described above. A high-speed video camera documented a small rolling movement during the treatment of the particles, held in place by the vacuum system, caused by the laminar flow that passed through them. This movement of the particles is probably beneficial for a complete coverage of the particles with a homogenous coating. SEM analyses were carried out on untreated and plasma treated Al_2O_3 microspheres; as shown in Figure 3, no noticeable differences were observed, attesting that the treatments performed resulted in negligible morphological changes.

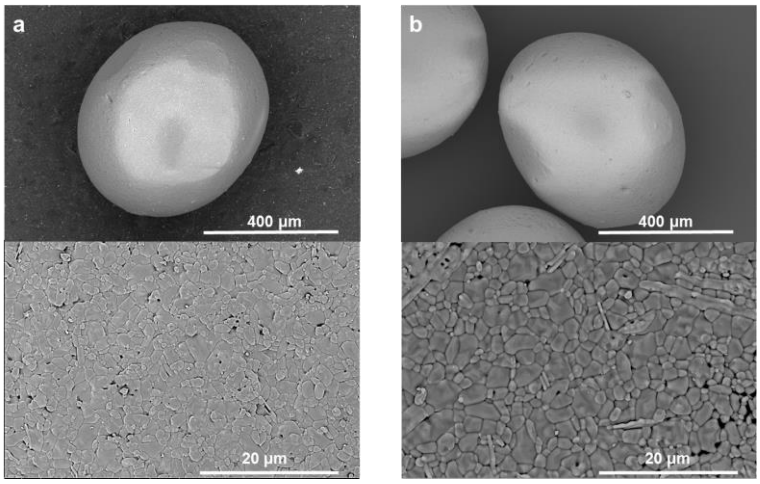

Figure 3. SEM analysis on the external surface at 150x (up) and 2500x of magnification of: a) untreated and b) plasma treated (f = 1.5 kHz, N_2 gas flow: 20 slm, N_2 aerosol flow: 1 slm, 60 passes, 200 W) microspheres, sintered at 1650°C for 1 h.

A normalized adsorption FT-IR spectrum of a coating plasma deposited (200 passes, i.e. 17 min total treatment time) on double polished silicon is shown in Figure 4. The plasma treated samples exhibit a signal in the area relative to the stretching of OH and NH groups (3300 cm^{-1}), the bands around 2900 cm^{-1} relative to CH stretching and a small band at 2180 cm^{-1} attributable to SiH stretching. The band with the maximum at 1672 cm^{-1} is due to the formation of amide C=O, C=C and NH groups. Since it is quite broad, the presence of acid C=O stretching (1723 cm^{-1}) can be assumed. The shoulder around 1500 cm^{-1} is attributable to primary and secondary amides. The bands around 1400 cm^{-1} are related both to CH bending and to CN stretching. Furthermore, the

spectrum presents the typical siloxane bands correlated with the Si-O-Si networking improvement (1053 cm^{-1}) and the Si-OH bending (934 cm^{-1}). The FT-IR spectrum demonstrates the presence of features characteristic of the APTES precursor (i.e. Si-O-Si and amines) in the coating. Moreover, the presence of additional chemical groups not present in the APTES structure, like OH and carbonyl, can be attributed to additional fragmentation and reaction of active species in the plasma phase or to post-oxidation reactions occurring when the coatings are exposed to air. Finally, the amide groups can be attributed both to the formation of new species during the process and to oxidation of amine groups upon air exposure.

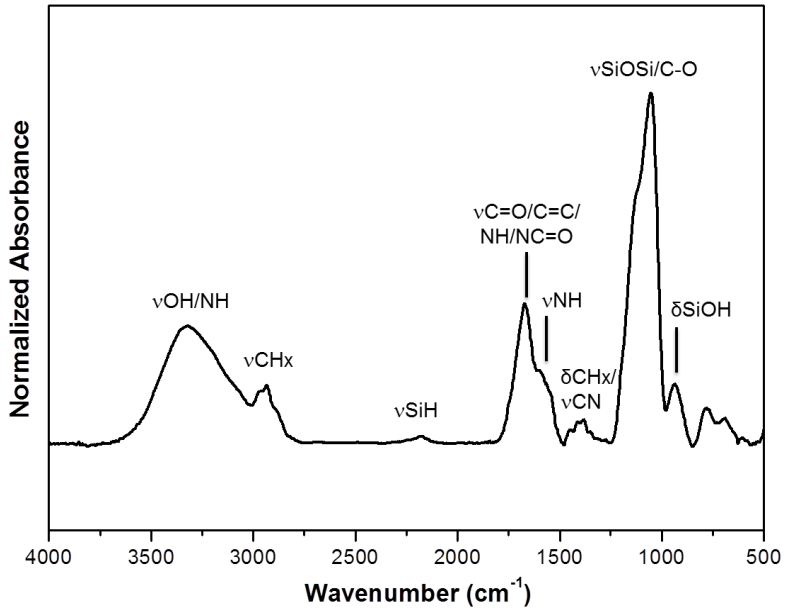

Figure 4. FT-IR spectra of plasma deposited APTES coating on double polished silicon (f = 1.5 kHz, N_2 gas flow: 20 slm, N_2 aerosol flow: 1 slm, 200 passes, 200 W).

The chemical composition of the outermost layer of the plasma deposited coatings was analyzed by XPS, on untreated and plasma treated Al_2O_3 microspheres sintered at 1650°C. The resulting atomic percentage of C, N, O, Al and Si is reported in Table 2. After the plasma treatment, the surface composition of Al_2O_3 changed with respect to the untreated one. Indeed N, Si and more C have been detected, with a decrease of Al and O. In order to evaluate the effect of the deposition time, the APTES coating was deposited in the experimental condition described in Table 1 (f = 1.5 kHz, N_2 gas flow: 20 slm, N_2 aerosol flow: 1 slm, 200 W), comparing the plasma treatments with

10, 30, and 60 passes. A decrease of the Al percentage is evident when the number of passes is increased from 10 to 60. This trend may either point out that 10 passes are not enough to homogeneously coat the microparticles with the coating, or that after 10 passes the coating is thinner than the XPS sampling depth (~10 nm). The HAADF-STEM and EDX analysis reported hereinafter can confirm such finding. In order to evaluate the effect of power, the process at 60 passes was realized both at 200 W and 400 W by keeping the other parameters constant (f = 1.5 kHz, N_2 gas flow: 20 slm, N_2 aerosol flow: 1 slm). As expected, increasing the input power leads to a loss of the carbon organic portion of the coating, with the consequent increment of the inorganic Si-O content. This behavior is commonly found also in LP plasma processes.[47] However, no relevant differences are observed in terms of Al percentage. When N_2 is replaced with Ar as carrier gas (f = 1.5 kHz, Ar gas flow: 20 slm, Ar aerosol flow: 1 slm, 60 passes, 50 W), it is interesting to note that the N/Si ratio decreases from 0.76 ± 0.03 to 0.61 ± 0.06, pointing out an involvement of nitrogen during plasma processing and growth of the deposited film. Furthermore, a less efficient surface coverage (high Al%) is observed with Ar as carrier gas with respect to N_2. A plasma discharge carried out only with N_2, without APTES, resulted ineffective in promoting grafting of nitrogen containing groups, as attested by the very low nitrogen content on the samples.

Looking at the elemental composition (%) of the plasma processed microspheres, it could also be pointed out that the C/Si ratios are always lower than 6, whatever the experimental conditions used. These values are less than the theoretical 9.14 C/Si ratio characteristic of the APTES precursor. This means that the fragmentation of the APTES precursor in the plasma process tends to eliminate its carbon-rich moieties, resulting in the deposition of coatings richer in Si and N moieties, as observed in the FT-IR spectra.

Table 2. Elemental composition (%) for untreated and plasma treated Al_2O_3 microspheres (Table 1) compared with theoretical values of the APTES precursor.

	C	**N**	**O**	**Al**	**Si**
APTES (theoretical)	64	7	21	-	7
Al_2O_3 (untreated)	8.8±0.2	0	52.5±0.02	38.7±0.2	0
10 passes, 200 W, N_2	41.5±3.7	6.0±1.0	31.4±0.2	11.7±2.9	9.5±1.0
30 passes, 200 W, N_2	57.1±0.6	8.0±0.1	24.5±0.6	1.1±0.3	9.3±0.1
60 passes, 200 W, N_2	52.5±0.1	8.3±0.1	27.6±0.4	0.6±0.2	10.9±0.4
60 passes, 400 W, N_2	45.2±0.5	8.8±0.2	32.5±0.4	0.8±0.1	12.7±0.1
60 passes, 50 W, Ar	53.3±0.1	6.8±0.7	26.9±0.2	1.9±0.6	11.1±0.1
60 passes, 200 W, N_2 (no monomer)	16.2±1.9	0,2±0.1	45.9±1.1	36.8±0.8	0

A deeper investigation of the coating chemical changes was carried out comparing the shape of the C1s and N1s high-resolution spectra, as a function of the experimental conditions used. The components considered for the best fitting of the spectra are listed in the experimental section. In Figure 5a, a broadening of the C1s peak is observed at highest BE when the input power is increased from 200 to 400 W (f = 1.5 kHz, N_2 gas flow: 20 slm, N_2 aerosol flow: 1 slm, 60 passes), in the zone relative to C=O and NC=O groups. No differences are observed, instead, for the N1s peaks. Therefore, the C1s broadening can be correlated with a higher surface density of carbonyl groups on microspheres treated at higher input power. Evaluating the influence of the two different carriers gas, in Figure 5b, the broadening of the C1s peak at high BE and the shift of the N1s peak toward high BE can be observed when N_2 is used as carrier instead of Ar, attesting to a higher surface density of amide groups. As reported above, using N_2 as carrier gas results in a coating with a higher density of nitrogen-containing moieties. In particular, as obtained from the best fitting (Figure S1), a surface atomic percentage of amine groups of 3.8% is reached with N_2, while with Ar carrier only 3.0% is achieved. This is an important result, considering that N_2 is a cheaper carrier gas compared with Ar, in particular in sight of the possible industrial scale-up of the process.

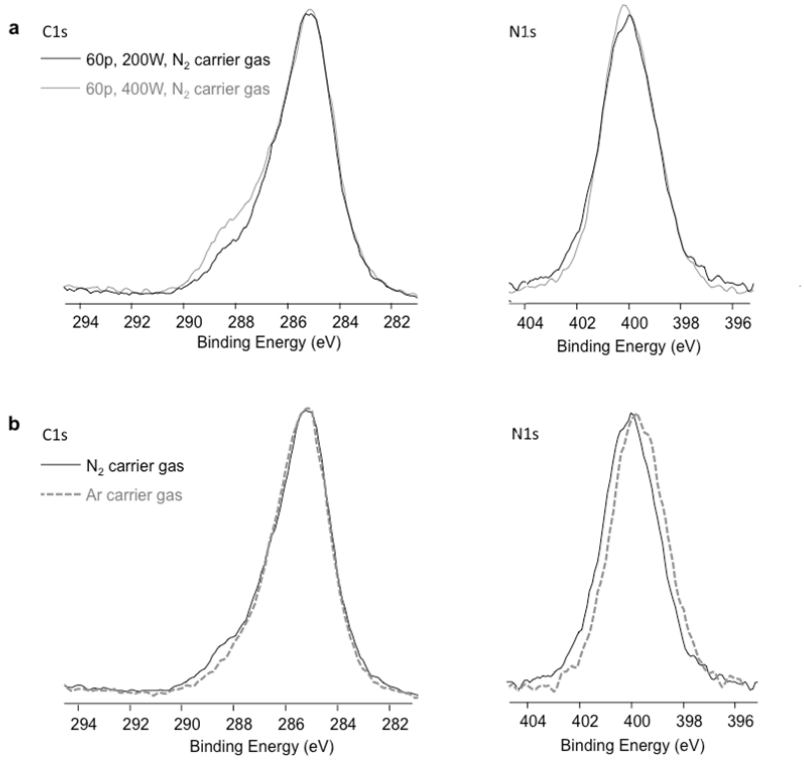

Figure 5. Overlaps of the C1s and N1s high resolutions spectra for plasma treated Al_2O_3 microspheres as a function of: a) input power values and b) carriers gas (experimental conditions in Table 1)

To confirm such findings, the amount of exposed primary amine groups on the coating obtained using N_2 as carrier gas (f = 1.5 kHz, N_2 gas flow: 20 slm, N_2 aerosol flow: 1 slm, 60 passes, 200 W) was estimated using Acid Orange dye, as discussed in the experimental section. For the plasma processed microspheres the density of amino groups found with this method was three times higher than the untreated samples: $156 \pm 15 \times 10^{15}$ (sites/g) against $49 \pm 4 \times 10^{15}$. The quite high density found on the untreated spheres is clearly a consequence of the non-specific adsorption of the dye, enhanced by the morphology of the samples. The comparison between the untreated and the plasma treated particles, however, confirms the presence of amino groups within the plasma coating, as supported by the XPS results, and provides an estimate of their density.

HAADF-STEM and EDX analyses were performed on Al_2O_3 microspheres sintered at 1650°C, in order to investigate the homogeneity of the coating on their external surface as a function of deposition time. Figure 6 shows the elemental maps acquired at the interface between the epoxy resin and Al_2O_3. A non-homogeneous coating is clearly observed in Figure 6a, corresponding to a

10 passes process. The samples treated for 30 and 60 passes (Figure 6b, c) present a more uniform film, with a thickness of approximately 50 nm. The obtained results explain why Al was detected by means of XPS on plasma processed samples, highlighting the increased homogeneity in terms of covered area of the microspheres when longer process times are utilized.

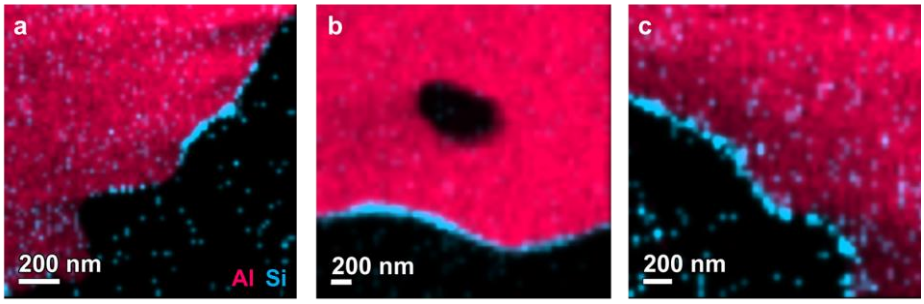

Figure 6. EDX elemental maps of Si and Al from FIB lamella of plasma treated microspheres produced at 1650°C of sintering temperature (f = 1.5 kHz, N_2 gas flow: 20 slm, N_2 aerosol flow: 1 slm, 200 W) after: a) 10, b) 30, c) 60 passes.

For the microspheres sintered at 1300°C, instead, the effect of the treatment time was evaluated as a function of the penetration depth of the coating into the porous structure, comparing normalized line profiles for the detected Si signal, perpendicular to the interface. The high signal to noise ratio reported in Figure 7 is due to the presence of a very thin coating, if compared to the width of the microspheres. Furthermore, in the EDX spectra a small but clear peak for Si is observed, while no peak for Si is detected in the area of the epoxy (black area) on top of the particles. This suggests that the presence or absence of Si can be distinguished, giving an idea of the qualitative assessment of the coating distribution into the porous structure of the particles. Indeed, as shown in Figure 7a for the sample treated by 10 passes Si is predominantly present at the interface. For the samples treated by 30 passes (Figure 7b), Si is observed in the pores close to the interface. After 60 passes (Figure 7c), it can be seen that the Si penetrates further inside, reaching an estimated depth of approximately 1 μm.

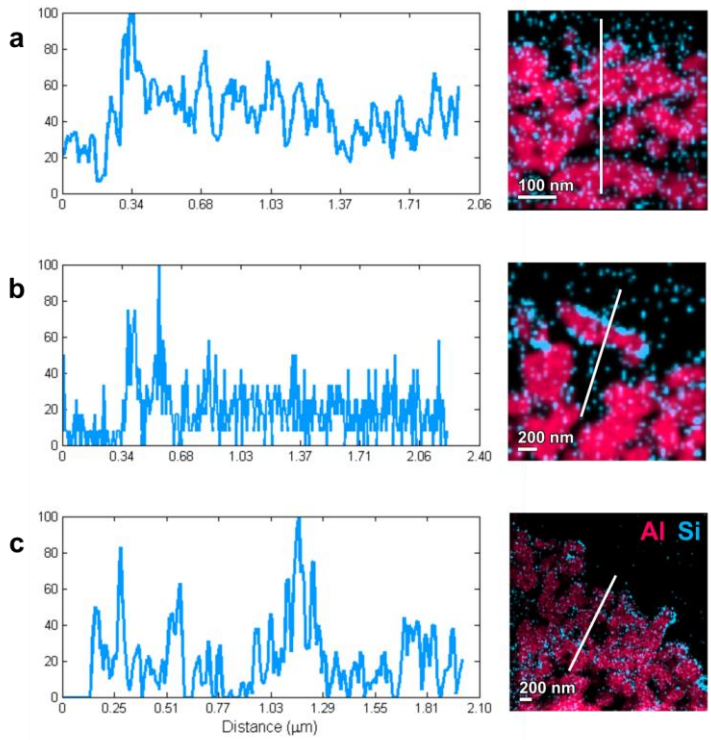

Figure 7. Intensity of the Si signal in function of the distance from the interface, along the white line indicated in the elemental maps of FIB lamella, for plasma treated microspheres produced at 1300°C of sintering temperature (f = 1.5 kHz, N_2 gas flow: 20 slm, N_2 aerosol flow: 1 slm, 200 W) after: a) 10, b) 30, c) 60 passes.

In order to evaluate the effect of the input power applied, the plasma processes performed at 200 W and 400 W were compared. The elemental maps in Figure 8b show that the sample treated at 400 W presents a uniform film at the interface. However, the coating seems to penetrate less inside the pores of the particle, compared with the sample treated at lower power value (Fig. 8a). It can thus be stated that the variation of power, in addition to affecting the chemical composition of the coating, as observed with XPS, has an influence also on the degree of diffusion of active species produced in the plasma phase into the porous structure of the microspheres.

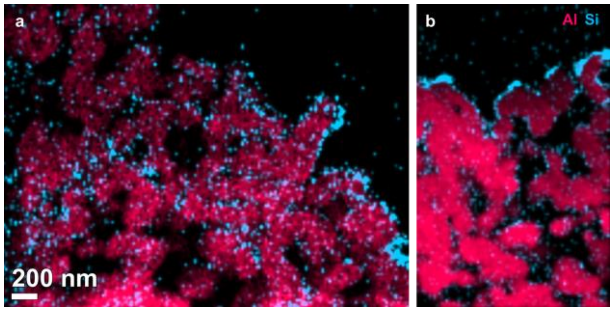

Figure 8. EDX elemental maps of Si and Al from FIB lamella of plasma treated microspheres (f = 1.5 kHz, N_2 gas flow: 20 slm, N_2 aerosol flow: 1 slm, 60 passes) at 200 W (a) and 400 W (b).

4 Conclusion

The vibrational droplet coagulation technique was used in order to shape monodisperse Al_2O_3 microspheres, with two different levels of porosity. These particles were surface modified with an atmospheric pressure plasma deposition process in a parallel-plate DBD reactor. APTES was used as precursor to obtain an aminosilane functional coating at the surface of the particles. This approach is presented as a feasible and convenient alternative to conventional wet chemistry methods, in terms of a notable reduction of overall process time and of liquid waste. The chemical composition of the thin plasma deposited film was optimized and the effect of the main external plasma parameters (treatment time, input power, carrier gas) was evaluated, in relation to both chemical composition and morphology of the coating. FT-IR analysis showed that the functional groups of the coupling agents are preserved. The treatment efficiency was demonstrated with XPS analysis and with a colorimetric assay, showing up to 9% of atomic nitrogen and confirming the presence of amino groups (3,8% of surface atomic concentration). Furthermore, FIB was used to prepare lamellar cross sections of the resin embedded microspheres. HAADF-STEM and EDX have offered an effective approach to evaluate the presence of the coating at the surface and into the pores of the microspheres; after 5 minutes of exposition to plasma, the particles resulted uniformly coated with a 50 nm thick layer of aminosilane coating, with about 1 μm of penetration depth of the coating inside the pores. It is important to highlight how the plasma process performed resulted effective, in minutes, in homogeneously processing the alumina microspheres, in much less time

with respect to conventional wet functionalization processes. Furthermore, the use of N_2 carrier in the process may be advantageous with respect to the use of more expensive carrier gases, in view of the up-scaling of this process in dynamic conditions, for increasing the efficiency of the method and the volume of the microspheres to be treated.

Acknowledgements

The technical assistance of the VITO staff (Materials Dpt) is gratefully acknowledged, especially D. Havermans, E. Van Hoof, R. Kemps (SEM-EDX) and A. De Wilde (Hg Porosimetry). Dr. S. Mullens and Dr. G. Scheltjens are kindly acknowledged for constructive discussions. SIM (Strategic Initiative Materials in Flanders) is gratefully acknowledged for its financial support. This research was carried out in the framework of the SIM-TRAP program (Tools for rational processing of nano-particles: controlling and tailoring nanoparticle based or nanomodified particle based materials). N. Claes and S. Bals acknowledge financial support from European Research Council (ERC Starting Grant #335078-COLOURATOM).

Keywords: alumina porous microspheres; aminosilane; atmospheric pressure glow discharges (APGD); powders functionalization, transmission electron microscopy (TEM)

Table of Contents/Graphical Abstract

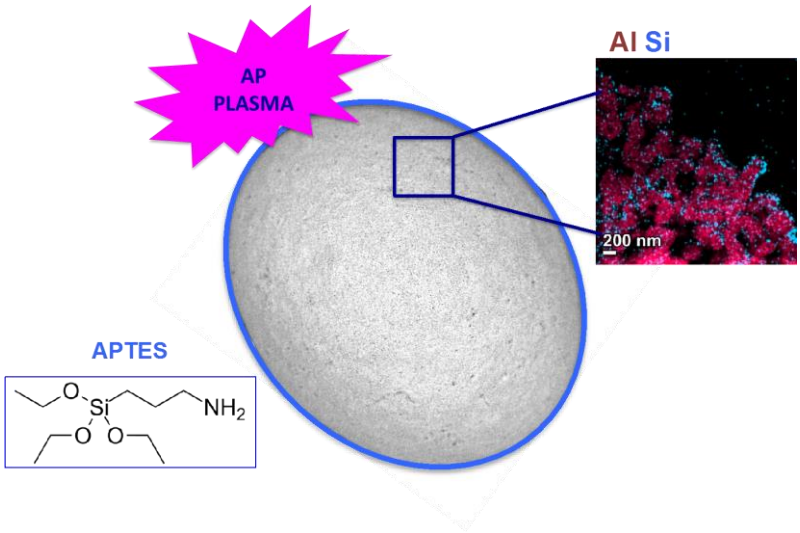

An atmospheric pressure DBD process is developed for the deposition of 3-Aminopropyltriethoxysilane coatings, Al_2O_3 porous microspheres at the external surface as well as within the pores. The successful functionalization with amino groups is verified. After 5 minutes of samples exposure to plasma, a uniform 50 nm thick plasma coating is obtained on the external surface of particles and reaches 1 μm of effective penetration depth inside the pores.

References

[1] V.D. Chaube, S. Shylesh, A.P. Singh, Journal of Molecular Catalysis A: Chemical 2005, 241, 79.
[2] D. Beiknejad, J Porous Mater 2013, 20, 1075.
[3] J. Wang, Z. H. Hu, Y. X. Miao, W. C. Li, Gold Bull 2014, 47, 95.
[4] A. Comite, E. S. Cozza, G. Di Tanna, C. Mandolfino, F. Milella, S. Vicini, Progress in Organic Coatings 2015, 78, 124.
[5] E.C. Hammel, O.L.R. Ighodaro, O.I. Okoli, Ceramics International 2014, 40, 15351.
[6] S. Akamine, M. Fujita, Journal of the European Ceramic Society 2014, 34, 4031.
[7] A. Szegedi, M. Popov, I. Goshev, J. Mihaly. Journal of Solid State Chemistry 2011, 184, 1201
[8] Z. Yi, L. F. Dumée, C. J. Garvey, C. Feng, F. She, J. E. Rookes, S. Mudie, D. M. Cahill, L. Kong, Langmuir 2015, 31, 8478.
[9] E. Xifre-Perez, J. Ferre-Borull, J. Pallares, L. F. Marsal, Mesoporous Biomaterials 2015, 2, 13

[10] Y. Wang, Q. Zhao, N. Han, L. Bai, J. Li, J. Liu, E. Che, L. Hu, Q. Zhang, T. Jiang, S. Wang, Nanomedicine: Nanotechnology, Biology, and Medicine 2015, 11, 313.
[11] Á. B. Sifontes, B. Gutierrez, A. Mónaco, A. Yanez, Y. Díaz, F. J. Méndez, L. Llovera, E. Cañizales, J. L. Brito, Biotechnology Reports 2014, 4, 21.
[12] A. A. Derakhshan, L. Rajabi, Powder Technol. 2012, 226, 117.
[13] E. P. Plueddemann, In Siloxane Coupling Agents, 2nd edition, Plenum Press, New York, USA 1991.
[14] S. Araki, H. Doi, Y. Sano, S. Tanaka, Y. Miyake, Journal of Colloid and Interface Science 2009, 339, 382.
[15] S. Zhao, L. S. Schadler, H. Hillborg, T. Auletta, Composites Science and Technology 2008, 68, 2976.
[16] S. Kangoa, S. Kaliab, A. Celli, J. Njugunad, Y. Habibie, R. Kumara, Progress in Polymer Science 2013, 38, 1232.
[17] A. Szegedi, M. Popova, I. Goshev, J. Mihàly, Journal of Solid State Chemistry 2011, 184, 1201.
[18] A. Santos, G. Macías, J. Ferré-Borrull, J. Pallarés, L. F. Marsal, ACS Appl. Mater. Interfaces 2012, 4, 3584.
[19] R d'Agostino, P Favia, C Oehr, MR Wertheimer, Plasma Proc. Polym. 2005, 2, 7.
[20] G. Da Ponte, E Sardella, F Fanelli, R d'Agostino, P Favia, The European Physical Journal Applied Physics 2011, 56, 2, 24023
[21] P. Favia, N. De Vietro, R. Di Mundo, F. Fracassi, R. d'Agostino, Plasma Process. Polym. 2006, 3, 6.
[22] S. Put, C. Bertels, A. Vanhulsel, Surface & Coatings Technology 2013, 234, 76.
[23] G. Oberbossel, A. T. Güntner, L. Kündig, C. Roth, R. von Rohr, Plasma Process. Polym. 2015, 12, 3, 285.
[24] T. D. Michl, B. R. Coad, A. Hüsler, K. Vasilev, H. J. Griesser, Plasma Process. Polym. 2015, 12, 4, 305.
[25] V. O. Kollath, S. Put, S. Mullens, A.Vanhulsel, J. Luyten, K. Traina, R. Cloots, Plasma Process. Polym. 2015, 12, 6, 594.
[26] B. Akhavan, K. Jarvis, P. Majewski, Powder Technology 2013, 249, 403.
[27] Y. Sawada, M. Kogoma, Powder Technology 1997, 90, 245.
[28] S. J. P. McInnes, T. D. Michl, B. Delalat, S. A. Al-Bataineh, B. R. Coad, K. Vasilev, H. J. Griesser, N .H. Voelcker, ACS Applied Materials & Interfaces 2016, 8, 4467.
[29] Z. Szalay, K. Bodišová, H. Pálková, P. Švančárek, P. Ďurina, J. Ráhel, A. Zahoranová, D. Galusek, Ceramics International 2014, 40, 12737.
[30] A. Solís-Gómez, M. G. Neira-Velázquez, J. Morales, M. A. Sánchez-Castillo, E. Pérez, Colloids and Surfaces A: Physicochem. Eng. Aspects 2014, 451, 66.
[31] D. Shi, P. He, S. X. Wang, W. J. van Ooij, L. M. Wang, J. Zhao, Z. Yu, J. Mater. Res., 2002, 17, 5.
[32] G. Da Ponte, A. K. Ghosh, A. Kakaroglou, D. Van Hemelrijck, B. Van Mele, B. Verheyde, Plasma Process. Polym. 2015, 12, 347.
[33] S. B. Said, F. Arefi-Khonsari, J. Pulpytel, Plasma Process. Polym. 2016, DOI: 10.1002/ppap.201600079.
[34] S. H. Jung, S. M. Park, S. H. Park, S. D. Kim, Ind. Eng. Chem. Res. 2004, 43, 5483.
[35] M Lazghab, K. Saleh, P. Guigon, Engineering research and design 2010, 8, 8, 686.
[36] J.L.H. Chau, C. C. Yang, Journal of Experimental Nanoscience 2014, 9, 4, 357.
[37] A. Choukourov, I. Melnichuk, A. Shelemin, P. Solař, J. Hanuš, D. Slavínská, H. Biederman, J. Phys. Chem. C 2015, 119, 28906.
[38] U. Roland, F. Holzer, A. Pöppl, F.-D. Kopinke, Applied Catalysis B: Environmental 2005, 58, 227.

[39] J. Gao, X. Zhu, Z. Bian, T. Jin, J. Hu, H. Liu, Microporous and Mesoporous Materials 2015, 202, 16.
[40] J. Pype, B. Michielsen, E.M. Seftel, S. Mullens, V. Meynen, Journal of the European Ceramic Society, 2017, 37, 189.
[41] J. Bour, J. Bardon, H. Aubriet, D. Del Frari, B. Verheyde, R. Dams, D. Vangeneugden, D. Ruch, Plasma Process. Polym. 2008, 5, 788.
[42] E. Lecoq, D. Duday, S. Bulou, G. Frache, F. Hilt, R. Maurau, P. Choquet, Plasma Process. Polym. 2013, 10, 250.
[43] N. Graf, E. Yegen, T. Gross, A. Lippitz, W. Weigel, S. Krakert, A. Terfort, Z. E. S. Unger, Surf. Sci. 2009, 603, 2849.
[44] S. Noel, B. Liberelle, L. Robitaille, G. De Crescenzo, Bioconjugate Chem. 2011, 22, 1690.
[45] A. A. Atia, A. M. Donia, W. A. Al-Amrani, Chemical Engineering Journal 2009, 150, 55.
[46] C. Dominguez, J. Chevalier, R. Torrecillas, G. Fantozzi, Journal of European Ceramic society 2001, 21, 381.
[47] M. Creatore, F. Palumbo, R. d'Agostino, P. Fayet, Surface and Coatings Technology 2001, 142, 163.